

Mott-Hubbard Transition on the Pyrochlore Lattice

Nyayabanta Swain^(a), Rajarshi Tiwari^(b) and Pinaki Majumdar^(a)

(a) *Harish-Chandra Research Institute,
Chhatnag Road, Jhusi, Allahabad 211019, India*

(b) *School of Physics and CRANN,
Trinity College, Dublin 2, Ireland*

(Dated: December 3, 2024)

The pyrochlore lattice involves corner sharing tetrahedra and the resulting geometric frustration is believed to suppress any antiferromagnetic order for Mott insulators on this structure. There are nevertheless short range correlations which could be vital near the Mott-Hubbard insulator-metal transition. We use a static auxiliary field based Monte Carlo to study this problem on reasonably large lattices, explicitly retaining all the spatial correlations. Our results reveal that increasing interaction drives the non magnetic metal to a ‘spin disordered’ metal with small local moments at some critical coupling and then to a large moment, gapped, Mott insulating phase at a stronger interaction. The spin disordered metal has a finite residual resistivity which grows with interaction strength, diverging at the upper coupling. We compare the temperature dependent resistivity obtained within our scheme to results on the pyrochlore iridates. Our approach captures the key qualitative features and the overall magnitude of the rather anomalous resistivity in this frustrated Mott system.

I. INTRODUCTION

The presence of geometric frustration disfavours long range antiferromagnetic order and promotes a complex magnetic state in insulating magnets with short range interaction^{1,2}. Two complications arise in magnetic insulators close to a Mott insulator-metal transition (IMT): (i) the ‘virtual hopping’ of the electrons mediate long range and multispin coupling, and (ii) the *magnitude* of the local moments weaken as the system is pushed towards the IMT. The first effect can lift the degeneracy of the short range model and promote an ordered state while the second tends to destroy the magnetic state altogether. The outcome of this interplay is lattice specific^{3,4}, of relevance to several real life materials, and requires tools beyond those usually applied in frustrated magnetism.

The possibilities in charge transport are also interesting. While the large moment, gapped, Mott phase is insulating, the strong suppression of the moment near the IMT, and possible orientational randomness due to frustration, can generate a spontaneously disordered magnetic background. This can lead to an electronic state with a pseudogap, an unusually large ‘residual’ resistivity^{5–7} and, possibly, anomalous Hall response if the moments organise in a non coplanar manner⁸.

The pyrochlores are a fascinating structure⁹ to explore these effects. In the deep Mott state on a pyrochlore lattice, where one expects only nearest neighbour antiferromagnetic coupling, the effective model can be written as a sum, over the tetrahedra, of squares of the ‘net moment’ in each tetrahedron^{10,11}. The minimum of this is infinitely degenerate since the four spins at the vertices of each tetrahedron just need to satisfy a zero vector sum. The appearance of longer range couplings as the electron-electron Hubbard repulsion reduces (or the bandwidth increases) can, potentially, lift the degeneracy and promote some ordered state. Whether it does so is not known. It is also not known whether the Mott transition on this structure would involve a direct transition from an insulator, with resistivity $\rho \rightarrow \infty$, to a metal with $\rho \rightarrow 0$, at zero temperature, or an extended crossover through some finite resistivity disordered magnetic state.

There are, remarkably, experimental realisations of Mott physics on the pyrochlore structure. These include the molybdates^{12–15}, $\text{Ln}_2\text{Mo}_2\text{O}_7$, and the iridates^{16–19}, $\text{Ln}_2\text{Ir}_2\text{O}_7$, where Ln is a rare earth ion. The Mo and Ir ions live on a pyrochlore lattice (while the Ln inhabit an interpenetrating pyrochlore structure). In addition to the Mott aspect the molybdates also involve double exchange ferromagnetism so we just focus on the iridates for now. The intriguing features in these are the following: (i) The strong coupling, small r_A , phase is supposed to have an ‘all-in/all-out’ (AIAO) magnetic configuration on the tetrahedra²⁰. (ii) The low temperature resistivity for some Ln suggests an unusually small gap, and for $\text{Ln}=\text{Nd}$ a highly resistive zero temperature state⁶. (iii) A material like $\text{Eu}_2\text{Ir}_2\text{O}_7$ that is insulating at ambient pressure can be driven ‘metallic’ by pressures $\sim \mathcal{O}(10\text{GPa})$ and the metallisation occurs through unusually resistive zero temperature states¹⁹. (iv) In a metallic system like $\text{Pr}_2\text{Ir}_2\text{O}_7$, with local moments on the Pr ion, the metallicity coexists with spin

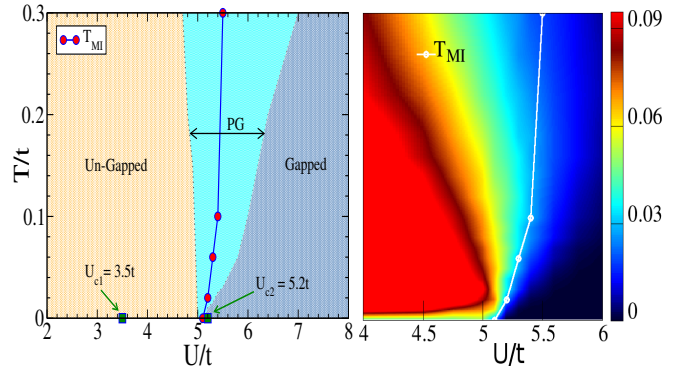


FIG. 1. Colour online: Phase diagram (left) and density of states at the Fermi level for varying U and T (right). Local moments appear at U_{c1} but the state remains metallic, turning insulating at U_{c2} . PG refers to a pseudogap state and the metal-insulator transition line separates regions with opposite signs of $d\rho/dT$. The right panel highlights the ‘re-entrant’ feature in the low energy DOS with increasing temperature.

liquid behaviour²¹ and an unconventional anomalous Hall response is observed⁸ - ascribed to possible spin chirality effect on the conduction electrons.

The iridates have a ‘simplifying’ feature in that the large spin-orbit coupling on Ir combines with the Hubbard effects to promote the AIAO magnetic state over a large part of parameter space. That allows the application of mean field theories to address the Mott problem. In this paper we consider the Mott transition on a pyrochlore lattice without including effects arising from SO coupling. That makes our study slightly distant from the real material. However, retaining the full pyrochlore degeneracy makes the problem conceptually interesting and, we observe, leads to a phenomenology for the Mott transition that is still useful for the iridates. We will report on the SO effects separately. We quickly survey the theory situation below before getting to our results.

(i) *Pyrochlore Heisenberg*: As the simplest case of an insulating antiferromagnet on this structure this model is well studied. For classical spins it has been established that there are no internal energy barriers between the degenerate minima, at $T = 0$, and no free energy barriers at finite T . There is no order at any temperature and there is no freezing transition either¹¹. In the semiclassical, $S \gg 1$, limit the classical degeneracy is partially lifted by the zero-point energy of quantum fluctuations but there remains an infinite manifold of degenerate collinear ground states²². The ground state for $S = 1/2$ is argued to be a quantum spin liquid²³.

(ii) *Pyrochlore Hubbard, without spin-orbit coupling*: For the half-filled Hubbard model on the pyrochlore the only work²⁴, we know of, not involving SO coupling suggests a Mott transition and a spin liquid Mott state, but detailed properties near the IMT are not available.

(iii) *Modeling the iridates*: (a) *Ab initio* calculations suggest that with increasing U one finds a metal, a topological semimetal with an ‘all-in/all-out’ magnetic configuration and finally a magnetic insulator²⁵. (b) The non-interacting model has a topological insulator (TI) and metallic phase, depending on the ratios of nearest neighbour hopping t and SO coupling λ . Mean field theory shows that the system undergoes successive transitions from a TI to a topological Weyl semi-metal (TWS) and to an ‘all-in/all-out’ magnetic insulator (AFI) as one increases U ^{26,27}. (c) Cluster DMFT calculations have shown transition from TI to an axion insulator state before the system goes to the TWS or AFI state²⁸.

We wish to address two broad questions in this paper, and more material specific (iridate) issues in a later submission involving SO coupling. The two questions are (i) What is the nature of the magnetic state as one moves towards weaker interaction in the Mott insulator, in particular what are the magnetic correlations near the IMT? (ii) What is the impact of these magnetic correlations on electron physics (resistivity, Hall response, optics, spectral features) near the IMT?

Our main results, using a real space static auxiliary field based Monte Carlo, are the following: (i) Increasing interaction in the ground state leads successively to an orientationally disordered small moment metal, then through a sharp crossover to a pseudogap phase, and finally to the gapped Mott insulator. (ii) In the pseudogap phase the electron system has

a finite but very high ‘residual’ resistivity and shows a negative temperature coefficient of resistivity (TCR). The resistivity trends compare well with measurements on the iridates. (iii) The low energy density of states has a strongly non monotonic temperature dependence over a wide interaction window near the MIT. Finally, (iv) The finite moment phases, from near the MIT to the deep Mott phase, are all disordered. Well in the Mott phase they display what seem to be power law (dipolar, pinch point) correlations that extend to a small finite temperature.

II. MODEL AND METHOD

We study the single band Hubbard model, with nearest neighbour hopping, on the pyrochlore lattice:

$$H = \sum_{ij,\sigma} (t_{ij} - \mu \delta_{ij}) c_{i\sigma}^\dagger c_{j\sigma} + U \sum_i n_{i\uparrow} n_{i\downarrow} \quad (1)$$

The $t_{ij} = -t$ for nearest neighbour hopping on the pyrochlore lattice and $U > 0$ is the Hubbard repulsion. We will set $t = 1$. The chemical potential μ is varied to maintain the electron density at $n = 1$ as the interaction and temperature T are varied.

We use a Hubbard-Stratonovich (HS) transformation³⁰ that introduces a vector field $\mathbf{m}_i(\tau)$ and a scalar field $\phi_i(\tau)$ at each site to decouple the interaction. This decomposition^{31,32} retains the rotation invariance of the Hubbard model, and hence the correct low energy excitations, and reproduces unrestricted Hartree-Fock (UHF) theory at saddle point.

We treat the \mathbf{m}_i and ϕ_i as classical fields, *i.e.*, neglect their time dependence, but completely retain the thermal fluctuations in \mathbf{m}_i . ϕ_i is treated at the saddle point level, *i.e.*, $\phi_i \rightarrow \langle \phi_i \rangle = (U/2) \langle \langle n_i \rangle \rangle = U/2$ at half-filling, since charge fluctuations would be penalised at temperatures $T \ll U$. Retaining the spatial fluctuations of \mathbf{m}_i allows us to estimate T_c scales, and access the crucial thermal effects on transport. We call this overall scheme the ‘static auxiliary field’ (SAF) approach, and have used it in the past to address the Mott transition on the triangular³³ and FCC³⁴ lattices. Others have used it successfully in superconductors³⁵, *etc.* We will discuss the limitations of this scheme later in the paper.

Within this approach the half-filled Hubbard problem is mapped on to electrons coupled to the field \mathbf{m}_i .

$$H_{eff} = \sum_{ij,\sigma} (t_{ij} - \tilde{\mu} \delta_{ij}) c_{i\sigma}^\dagger c_{j\sigma} - \frac{U}{2} \sum_i \mathbf{m}_i \cdot \vec{\sigma}_i + \frac{U}{4} \sum_i \mathbf{m}_i^2$$

where $\tilde{\mu} = \mu - \frac{U}{2}$. H_{eff} can be seen as comprising of an electronic Hamiltonian, H_{el} (the first two terms above) and the classical ‘stiffness’ cost $H_{cl} = \frac{U}{4} \sum_i \mathbf{m}_i^2$. The magnetic configurations $\{\mathbf{m}_i\}$ seen by the electrons follow the distribution

$$P\{\mathbf{m}_i\} \propto \text{Tr}_{cc^\dagger} e^{-\beta(H_{el} + H_{cl})}$$

Within the SAF scheme H_{eff} and $P\{\mathbf{m}_i\}$ define a coupled fermion-local moment problem. If the moments are large

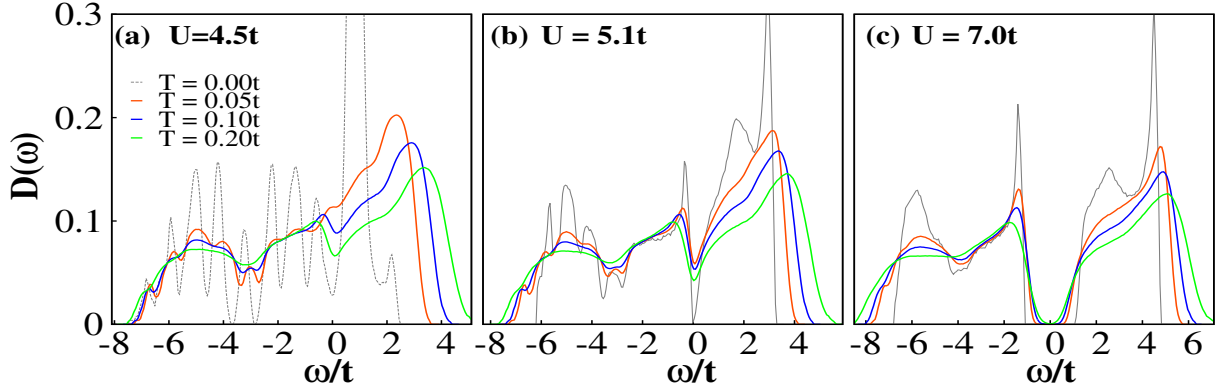


FIG. 2. Colour online: Density of states at $U/t = 4.5$, 5.1 and 7.0 with varying temperatures. $U/t = 4.5$ lies in the gap-less metallic side, $U/t = 7.0$ lies in the gapped Mott-insulating side, where as $U/t = 5.1$ corresponds to the pseudo-gap (PG) regime with a pronounced dip in the DOS at the Fermi-level.

and random the electronic problem requires numerical diagonalisation. Similarly, the $P\{\mathbf{m}_i\}$ cannot be written down in closed form since the fermion free energy is not known for arbitrary $\{\mathbf{m}_i\}$. The method of choice in these situations is a combination of Monte Carlo (MC) for updating the \mathbf{m}_i with exact diagonalisation (ED) of the fermion Hamiltonian for computing the Metropolis update cost.

To access large sizes within limited time, we use a cluster algorithm for estimating the update cost. The energy cost of updating the variable \mathbf{m}_i is computed by diagonalizing a cluster (of size N_c , say) constructed around the site \mathbf{R}_i . We have extensively benchmarked this ‘traveling cluster’ method³⁶. Results in this paper are obtained for lattices of 6^3 unit cells with 4 atoms per unit cell, using a cluster with $3^3 \times 4$ atoms.

From the equilibrium magnetic configurations we calculate the thermally averaged structure factor $S(\mathbf{q}) = \frac{1}{N^2} \sum_{ij} \langle \mathbf{m}_i \cdot \mathbf{m}_j \rangle e^{i\mathbf{q} \cdot (\mathbf{r}_i - \mathbf{r}_j)}$ at each temperature. The rapid growth of a mode at some $\mathbf{q} = \mathbf{Q}$ indicates the onset of order. Electronic properties are calculated by diagonalising H_{el} on the full lattice for equilibrium $\{\mathbf{m}_i\}$ configurations.

III. RESULTS

A. Phase diagram and magnetism

Fig.1, left panel, shows the $U - T$ phase diagram in terms of the magnetic, transport, and spectral properties that we observe. The following features emerge:

At $T = 0$ our MC annealing is equivalent to the minimization $\frac{\delta}{\delta \mathbf{m}_i} \langle H_{eff} \rangle = 0$. Upto a critical coupling $U_{c1} \sim 3.5t$ the minimisation leads to $m_i = |\mathbf{m}_i| = 0$ at all sites. As a result the electronic ground state is essentially tight binding, with the sharply suppressed DOS at Fermi level characteristic of pyrochlore band structure. For $U_{c1} < U < U_{mid}$ where $U_{mid} \approx 5t$ we observe a small moment, orientationally disordered, magnetic state. With the disorder caused by these moments the DOS at the fermi level gains weight. In a nar-

row region around U_{mid} there is rapid increase in the mean magnitude of the moments (shown in a later figure) and, as a result, the DOS at fermi level displays a sharp pseudogap (PG). At $U_{c2} \sim 5.2t$ the PG actually converts to a hard gap. For $U \gtrsim U_{c2}$ the moments are large and saturate as $U \rightarrow \infty$.

Since the moments do not have an obvious periodic pattern the only way to access the ground state is via Monte Carlo, *i.e*, employ an annealing based minimisation. The result of this is a ‘disordered’ magnetic state at all $U > U_{c1}$ (where moments first appear). This result is expected in the $U/t \rightarrow \infty$ limit where the short range Heisenberg model is applicable but its continuation down to the Mott transition was not obvious. It seems that even the longer range couplings at finite U/t do not lift the degeneracy sufficiently. The ‘disordered’ state however is not random but has power law correlations that lead to ‘pinch point’ singularities in the magnetic structure factor. These are characteristic of a classical spin liquid (CSL) state and we find that they survive down to $U/t \sim 8$. We will discuss them elsewhere.

At finite T thermal fluctuations of local moments in the weak coupling side ($U < U_{mid}$) quickly increases, resulting in an increase in the low energy DOS with temperature. In the strong coupling side ($U > U_{mid}$) the angular fluctuations of the local moments result in a slight reduction of the Mott-gap with temperature. However in the Mott-transition neighbourhood, $U_{mid} < U < U_{c2}$, thermal fluctuations of the local moments quickly widen the PG window as T increases.

We demarcate the finite T metal-insulator boundary in terms of the temperature derivative $d\rho/dT$. A state is metallic if $d\rho/dT > 0$ and insulating if $d\rho/dT < 0$. The spectral features and resistivity are discussed in detail further on.

B. Density of states

We compute the single particle DOS as $D(\omega) = \frac{1}{N} \langle \sum_n \delta(\omega - \epsilon_n) \rangle$ where the angular brackets indicate thermal average over equilibrium configurations. Fig.2 shows the thermal evolution of the DOS in three of the four broad inter-

action regimes of our phase-diagram.

(i) For $U < U_{c1}$ the ground state is characterized by $m_i = |\mathbf{m}_i| = 0$. The electron model reduces to the usual tight-binding pyrochlore lattice. This is characterised by two flat-bands at the upper band edge and vanishing DOS at the fermi-energy. At finite T small ‘randomly’ oriented local moments appear in the system broadening the flat bands and leading to a small DOS at the fermi level. (ii) For $U_{c1} < U < U_{mid}$, the ground state has small disordered local moments. The DOS is gapless and the weight at the fermi level is non-monotonic with T , increasing initially and then decreasing (with a weak PG form, see Fig.2.(a)). (iii) For $U_{mid} < U < U_{c2}$ the DOS has a PG at $T = 0$. This fills up initially with increasing T but deepens again above a temperature scale that is visible in Fig.1 right panel. (iv) For $U > U_{c2}$ the ground state has a hard gap. With increase in temperature, the angular fluctuations of the local moments result in a slight reduction of the Mott-gap, but an increase in the band width. However, there exists a clear Mott-gap till very high temperature, $T \sim O(U)$.

C. Transport and optics

We obtain the d.c. resistivity $\rho(T)$ via the low frequency limit of the optical conductivity $\sigma(\omega)$, computed through the Kubo formula³⁷.

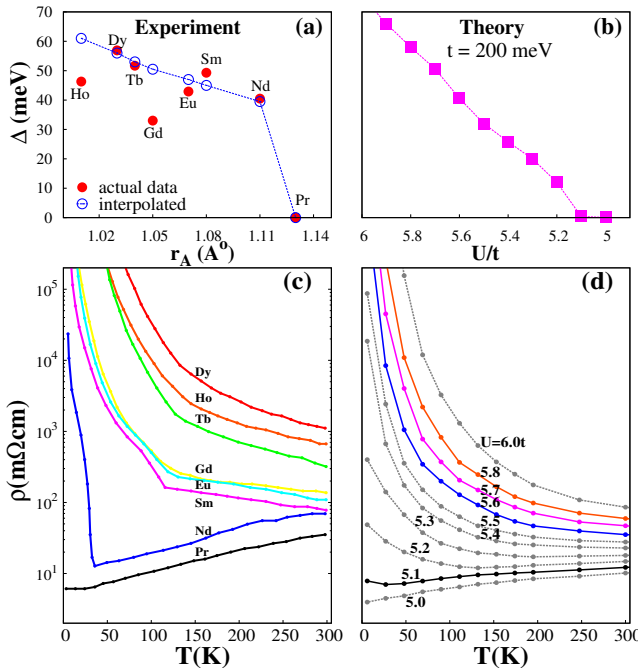


FIG. 3. Colour online: (a) Gap $\Delta(r_A)$ obtained from the low temperature resistivity of iridates by fitting to an activated behavior. (b) The gap $\Delta(U)$ obtained from theory, with the absolute value set by choosing $t = 200$ meV. Using $\Delta(U) = \Delta(r_A)$ allows us to obtain $U(r_A)$. The y range is identical in panels (a) and (b). (c) Resistivity in the iridates for varying rare earth. (d) Resistivity calculated within our scheme. The x and y axis limits are exactly the same in panels (c) and (d). The choice of t for the iridates is discussed in the text.

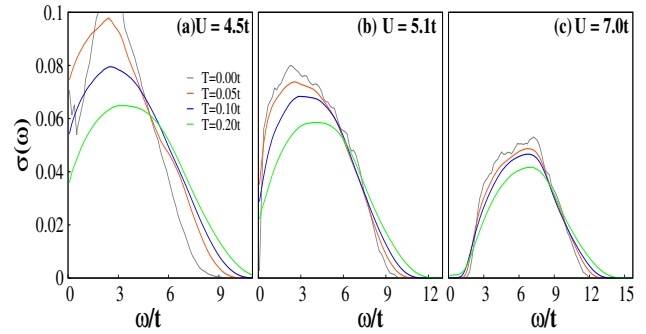


FIG. 4. Colour online: Optical conductivity at $U/t = 4.5, 5.1$ and 7.0 with varying temperatures. $U/t = 4.5$ shows a non-Drude like behavior with peak at small and finite frequency. With increasing U/t the peak moves to higher frequency and the zero frequency weight decreases continuously and eventually there appears a gap as $U/t \geq U_{c2}/t$.

Assuming that the iridates can be modeled within a single band Hubbard scheme³⁹, Fig.3.(a)-(b) show the calibration of the U values that are appropriate to the $\text{Ln}_2\text{Ir}_2\text{O}_7$ family. Panel (a) shows the low temperature gap extracted¹⁷ via a fit of the form $\rho(T) = \rho_0 e^{\Delta/T}$. This yields $\Delta(r_A)$ which has a somewhat non monotonic dependence. The blue dotted curve is a smooth (and piecewise linear) interpolation that we use to model the behaviour. Panel (b) shows the theoretically obtained low T gap $\Delta(U)$ plotted in absolute units for the choice $t = 200$ meV³⁸. The U value appropriate to a particular Ln is obtained by using $\Delta(U) = \Delta(r_A)$ (where we use the interpolated ‘experimental’ result). Panel 3(c) shows the experimentally obtained resistivity for the Ln family while 3(d) shows the theory based result for U values that are close to the specific Ln (they have the same colour). We first comment on some features in the theory result:

(i) For $U < U_{c1}$ the $T = 0$ resistivity $\rho(0) = \rho(T = 0) = 0$. This is the tight-binding semi-metallic regime of the pyrochlore lattice where the DOS vanishes linearly at the fermi-energy. We have $d\rho/dT > 0$ in this regime which can be understood in terms of a disorder induced density of states and the scattering of electrons from the disordered moments.

(ii) For $U > U_{c2}$ the system has a clear gap at $T = 0$. Thus $\rho(0) \rightarrow \infty$ with $d\rho/dT < 0$. This is the Mott-insulating regime.

(iii) Between U_{c1} and U_{c2} the residual resistivity $\rho(0)$ is finite with $d\rho/dT > 0$ for $U_{c1} < U < U_{mid}$ and $d\rho/dT < 0$ for $U_{mid} < U < U_{c2}$. This can be understood as the scattering of electrons from the background fluctuating local moments. As U increases, the average local moment magnitude $m_{av}(U)$ also increases, resulting in the increased scattering of the electrons and a depleting DOS at the fermi level.

The low T gaps in panel (c) and (d) are equal by construction but that by itself does not ensure that the theory predict a wide interaction window over which the resistivity is large and finite at $T = 0$ with $d\rho/dT < 0$. This theory prediction is indeed prominently visible in the Ln family, both in the ambient pressure compounds and also in situations of pressure driven metallisation. The absolute values of $T = 0$ resistiv-

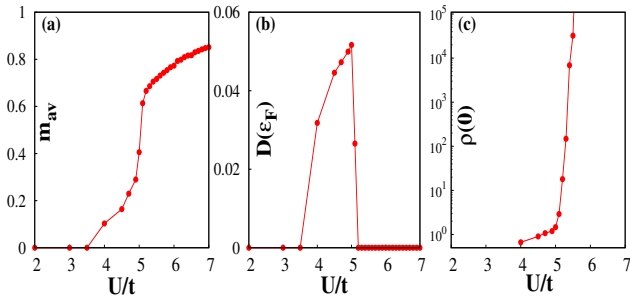


FIG. 5. Colour online: The variation with U/t of the average moment m_{av} , the density of states at the Fermi level, $D(\epsilon_F)$, and the resistivity $\rho(0)$, at $T = 0$

ity are somewhat smaller in our low U cases because we do not have any impurity scattering (unlike the real materials). Similarly, the high T values obtained from theory are lower than those in experiments because there is no electron-phonon scattering included in our theory.

Fig.4 shows the optical conductivity from our calculation as we go across the Mott transition point. The important points are: (i) $\sigma(\omega)$ for $U < U_{c1}$ will have a Drude peak at $\omega = 0$ for $T = 0$ due to the presence of 2 flats bands at the upper band edge. With increase in temperature, as small moments appear in the system the Drude peak will be shifted to small, finite ω . This is because the DOS for small $\omega \neq 0$ has higher weight compared to $\omega = 0$. $\sigma(\omega)$ for $U_{c1} < U < U_{mid}$ also shows similar behavior due to the presence of small moments.

(ii) For $U > U_{c2}$ the system has a clear gap $\Delta(T)$ in the DOS. Thus $\sigma(\omega) = 0$ for $\omega < \omega_c \sim \Delta(T)$. With increasing temperature the gap $\Delta(T)$ reduces, resulting in small, but increasing low frequency weight of $\sigma(\omega)$ and the peak position shifts to higher frequency. This Mott-insulating regime of the pyrochlore lattice may have finite spectral weight at $\omega = 0$ in the optical conductivity $\sigma(\omega)$ at high temperatures when $\omega \rightarrow \omega_c \sim \Delta(T)$.

(iii) For $U_{mid} < U < U_{c2}$ we have a pseudo-gap in the DOS. $\sigma(\omega = 0) \rightarrow 0$ in this regime. However with increasing temperature the zero frequency weight increases initially and then decreases in accord with the behavior of the DOS in this regime.

To better correlated the anomalous properties in the low T state near the IMT we have calculated the mean moment $m_{av} = \frac{1}{N} \sum_i \langle |\mathbf{m}_i| \rangle$ and show it along with the density of states at the fermi level, $D(\epsilon_F) = D(\omega/t = 0)$, and $\rho(0)$ in Fig.5.

IV. DISCUSSION

I. Methodology: Given the complexity of the pyrochlore Mott problem where both spatial and temporal fluctuations could be important near the Mott transition, we comment on some issues of method below.

(i) *Static approximation in the Monte Carlo:* Fully handling the temporal fluctuations of the \mathbf{m}_i fields, and the ϕ_i , requires a quantum Monte Carlo scheme. The absence of such results

is probably due to the sign problem for fermions in the frustrated geometry. However, it is possible, although non trivial, to set up a gaussian approximation for the finite Matsubara frequency components of the \mathbf{m}_i and the ϕ_i fields, while retaining the treating the $\Omega_n = 0$ mode exactly as we have. This is a project for the future. However, since the present theory itself predicts no order at any U or temperature, we do not expect the qualitative magnetic state to be modified. Incidentally, a C-DMFT calculation, retaining the full time dependence but restricted to a small cluster, yields results (for the SO coupling + Mott problem) that are qualitatively very similar to what we observe here. At high temperature our classical fluctuation approach should become a better and better approximation of the full theory.

(ii) *Finite size effects:* We have done our calculations on lattices that involve ~ 800 atoms. This is much larger than what is typically accessible in full fledged fermion QMC (since time fluctuations also have to be included), allowing us to access resistivity and spectral features which do not involve artificial broadening. It is possible to try the calculations on $8^3 \times 4$ lattices (involving about 2000 atoms) and checks at individual parameters do not reveal a significant difference.

(iii) *Cluster based update:* Our Metropolis update involves a small cluster rather than diagonalisation of the full Hamiltonian. This is well controlled in the large U limit when the ‘range’ of electron excursion is limited but less reliable near the Mott transition. For that purpose we have used a variational calculation, described below, that uses the MC result as an ansatz and checks the stability of such a state on large (upto $10^3 \times 4$ lattices) for the ground state. The results are discussed below - and are qualitatively consistent with the cluster based MC.

II. Variational calculation: Since MC hints that the magnetic ground state involves disordered local moments for $U > U_{c1}$ we tried a simple variational check. We set up trial configurations with randomly oriented but uniform magnitude \mathbf{m}_i , with the magnitude m_0 as a variational parameter. This differs from the real situation where the \mathbf{m}_i have some amplitude inhomogeneity and also orientational correlation. Minimisation confirms the presence of a small moment phase, beyond some U_{low} , with an initial slow growth of $m_0(U)$ and then a rapid crossover to large values at some U_{high} . The U_{low} and U_{high} are about 10% higher than MC estimates and may get reduced if spatial correlations are included. We will present the results of the variational check separately.

III. Relation to the real iridates: While our observation of a metal-insulator transition and transport results are consistent with experiments^{16,17} on the pyrochlore iridates, there are both qualitative and quantitative differences which merit discussion.

To make a correspondence with the iridates we consider only the 5d electrons arising from Ir^{4+} delocalising on the pyrochlore lattice. This would lead to a multiband description, but a consideration of crystal field effects³⁹ and SO coupling leads to an effective $j = 1/2$ level (and band) that is half-filled. This has been widely used in the literature, but, crucially, keeping the SO coupling which stabilises the AIAO order and gives it a finite T_c ⁴⁰.

In the absence of SO coupling we get a (classical) spin liquid state, rather than the observed AIAO. However, two features, the fall of T_{MI} with decreasing interaction, and the highly resistive zero temperature state, are already accessible without SO effects.

V. CONCLUSION

We have studied the Mott transition in half-filled Hubbard model on a pyrochlore lattice. The geometric frustration and the resulting degeneracy prevents the occurrence of any magnetic order in the deep Mott state, and this, surprisingly, continues all the way to the insulator-metal transition. Beyond the IMT there is a window with a pseudogap in the density of states, disordered local moments, and a large residual resistivity. These trends have a strong correspondence with transport results on the pyrochlore iridates.

We acknowledge use of the HPC clusters at HRI and discussions with Shubhro Bhattacharjee. PM acknowledges support from an Outstanding Research Investigator grant of the DAE-SRC.

¹ N. P. Ong and R. J. Cava, *Science*, **305**, 52 (2005).
² L. Balents, *Nature*, **464**, 199 (2010).
³ K. Kanoda, *J. Phys. Soc. Jpn.* **75**, 051007 (2006). B. J. Powell and R. H. McKenzie, *Rep. Prog. Phys.* **74**, 056501 (2011).
⁴ Y. Imai, N. Kawakami and H. Tsunetsugu, *Phys. Rev. B* **68**, 195103 (2003). N. Bulut, W. Koshiba and S. Maekawa, *Phys. Rev. Lett.* **95**, 037001 (2005).
⁵ M. M. Abd-Elmeguid, *et al.*, *Phys. Rev. Lett.* **93**, 126403 (2004).
⁶ K. Ueda, *et al.*, *Phys. Rev. Lett.* **109**, 136402 (2012).
⁷ Gia-Wei Chern, Saurabh Maiti, Rafael M. Fernandes and Peter Wolfe *Phys. Rev. Lett.* **110**, 146602 (2013).
⁸ Y. Machida, *et al.*, *Phys. Rev. Lett.* **98**, 057203 (2007).
⁹ J. S. Gardner, M. J. P. Gingras and J. E. Greedan, *Rev. Mod. Phys.* **82**, 53 (2010).
¹⁰ J. N. Reimers, *Phys. Rev. B* **45**, 7287 (1992).
¹¹ R. Moessner and J. T. Chalker, *Phys. Rev. B* **58**, 12049 (1998).
¹² B. D. Gaulin, J. N. Reimers, T. E. Mason, J. E. Greedan, and Z. Tun, *Phys. Rev. Lett.* **69**, 3244 (1992).
¹³ M. J. P. Gingras, C. V. Stager, N. P. Raju, B. D. Gaulin, and J. E. Greedan, *Phys. Rev. Lett.* **78**, 947 (1997).
¹⁴ S. Iguchi, *et al.*, *Phys. Rev. Lett.* **102**, 136407 (2009).
¹⁵ Y. Motome and N. Furukawa *et al.*, *J. Phys. Conf. Ser.* **320**, 012060 (2011).
¹⁶ D. Yanagishima and Y. Maeno, *J. Phys. Soc. Jpn.* **70**, 2880 (2001).
¹⁷ K. Matsuhira, *et al.*, *J. Phys. Soc. J.* **80**, 094701 (2011).
¹⁸ M. Sakata, *et al.*, *Phys. Rev. B* **83**, 041102 (2011).
¹⁹ F. F. Tafti, *et al.*, *Phys. Rev. B* **85**, 205104 (2012).
²⁰ Eric Kin-Ho Lee, Subhro Bhattacharjee and Yong Baek Kim *Phys. Rev. B* **87**, 214416 (2013).
²¹ S. Nakatsuji, *et al.*, *Phys. Rev. Lett.* **96**, 087204 (2006).
²² U. Hizi and C. L. Henley, *Phys. Rev. B* **80**, 014407 (2009).
²³ B. Canals and C. Lacroix, *Phys. Rev. Lett.* **80**, 2933 (1998).
²⁴ Satoshi Fujimoto, *Phys. Rev. B* **64**, 085102 (2001), *Phys. Rev. B* **67**, 235102 (2003).
²⁵ X. Wan, A. M. Turner, A. Vishwanath and S. Y. Savrasov, *Phys. Rev. B* **83**, 205101 (2011).
²⁶ W. Witczak-Krempa and Y. B. Kim, *Phys. Rev. B* **85**, 045124 (2012).
²⁷ William Witczak-Krempa, Ara Go and Yong Baek Kim, *Phys. Rev. B* **87**, 155101 (2013).
²⁸ Ara Go, William Witczak-Krempa, Gun Sang Jeon, Kwon Park and Yong Baek Kim *Phys. Rev. Lett.* **109**, 066401 (2012).
²⁹ S. V. Isakov *et al.*, *Phys. Rev. Lett.* **93**, 167204 (2004), C. L. Henley, *Phys. Rev. B* **71**, 014424 (2005).
³⁰ R. L. Stratonovich, *Sov. Phys. Doklady* **2**, 416 (1958), J. Hubbard, *Phys. Rev. Lett.* **3**, 77 (1959).
³¹ J. Hubbard, *Phys. Rev. B* **19**, 2626 (1979).
³² H. J. Schulz, *Phys. Rev. Lett.* **65**, 2462 (1990).
³³ R. Tiwari and P. Majumdar, *Euro Phys. Lett.* **108**, 27007 (2014).
³⁴ R. Tiwari and P. Majumdar, *arXiv:1302.2922v1* (2013).
³⁵ Y. Dubi, Y. Meir and Y. Avishai, *Nature*, **449**, 876 (2007).
³⁶ S. Kumar and P. Majumdar, *Eur. Phys. J. B*, **50**, 571 (2006).
³⁷ P. B. Allen in *Conceptual Foundation of Materials* V.2, edited by Steven G. Louie, Marvin L. Cohen, Elsevier (2006).
³⁸ Choong H. Kim, *et al.*, *Phys. Rev. Lett.* **108**, 106401 (2012).
³⁹ B. J. Kim, *et al.*, *Phys. Rev. Lett.* **101**, 076402 (2008).
⁴⁰ M. Elhajal, B. Canals, R. Sunyer and C. Lacroix, *Phys. Rev. B* **71**, 094420 (2005).